

Nature of star formation in first galaxies

Mahavir Sharma 

Indian Institute of Technology (IIT) Bhilai, GEC Campus, Sejbahar, Raipur, 492015, India
email: mahavir@iitbhilai.ac.in

Abstract. One of the primary foci of research in astrophysics is on developing a rigorous understanding of the first galaxies. This entails studying the physical processes such as accretion, cooling and star formation in first galaxies, and also investigating the consequences of these processes in the present day Universe. We investigate the star formation in the early galaxies and its subsequent evolution using the EAGLE simulation and find that the star formation has a smooth evolutionary behaviour at low redshifts leading to a main sequence of star formation that can be explained by deterministic models using accretion history as an input. In contrast, at high redshift (> 6), most of the galaxies are bursty. At high redshift, instead of exhibiting a main sequence in $\text{SFR} - M_{\text{h}}$ plane, they bunch-up around a halo mass of $\approx 10^9 M_{\odot}$ and $\text{SFR} \approx 0.1 M_{\odot} \text{ yr}^{-1}$. As a consequence, the reionization of the Universe is led by low mass haloes hosting brighter galaxies that are undergoing intense bursts. Furthermore, the bursts in the infant galaxies lead to a poorly mixed interstellar medium in which the stars can form from gas enriched predominantly by a single nucleosynthetic channel. The lower mass subset of the stars formed in first galaxies resemble the carbon enhanced metal poor stars in our Galaxy while the higher mass ones reionized the Universe.

Keywords. galaxies: high-redshift, galaxies: formation, galaxies: evolution, stars: abundances, ISM: structure, ISM: evolution

1. Introduction

The Universe plunged into the dark ages after the electrons recombined with protons at redshift $z \approx 1100$, that is also known as the surface of last scattering when the cosmic microwave background photons were emitted. During the dark ages the primordial perturbations in the neutral hydrogen in the Universe kept on evolving (e.g. [Dodelson 2003](#)). How exactly the first stars and galaxies emerged out of the growing density perturbations is a challenge to the 21st century astrophysics (e.g. [Bromm 2013](#); [Naab & Ostriker 2017](#)).

At the observational front, there has been a quest to detect the first galaxies using state of the art instruments such as the Hubble Space Telescope ([Beckwith et al. 2006](#)). The James Webb Space Telescope (JWST) ([Gardner et al. 2006](#)) is also expected to provide vital information on the first galaxies, such as their star formation rates (SFRs) and the nebular emission lines from them. Furthermore, the Universe was not completely dark during the dark ages, since the neutral hydrogen can be seen through its hyperfine spin-flip 21 cm transition (e.g. [Pritchard & Loeb 2012](#)). Detecting the 21 cm signal from the early Universe is a primary focus of the mega radio astronomy projects such as the Low Frequency Array ([van Haarlem et al. 2013](#)), the Murchison Widefield Array (e.g. [Beardsley et al. 2019](#)) and the upcoming Square Kilometre Array ([Weltman et al. 2020](#)). A significant effort in this direction is devoted to detect the progress of the Universe during the epoch when it is undergoing a transition from the dark neutral to the bright ionized state. This transition known as the ‘cosmic reionization’ was brought about by the star formation in first galaxies.

Theoretical effort has focused on simulating the formation of the first galaxies (Schaye et al. 2015; Crain et al. 2015; Vogelsberger et al. 2014; Naab & Ostriker 2017). Another step in this direction was to deploy the outcomes of galaxy formation into a radiative transfer calculation in the evolving Universe to reproduce the progress of reionization and to predict the evolving power spectrum of the 21-cm signal (e.g. Sokasian et al. 2001; Santos et al. 2010; Wise et al. 2014; Mesinger et al. 2011).

Therefore, an accurate modelling of the formation of galaxies and stars lies at the heart of the current problems in cosmology. Understanding their evolution to the present day has also been a major theme of research, and an objective of the milestone computational efforts such as the MILLENNIUM simulation (Springel et al. 2005) and more recently the EAGLE (Schaye et al. 2015; Crain et al. 2015; McAlpine et al. 2016) and ILLUSTRIS simulation (Vogelsberger et al. 2014). These computational studies do an excellent job in reproducing the galaxy luminosity functions and the stellar mass to halo mass relations. They can reproduce the evolutionary history of cosmic star formation, and also do very well in reproducing the quenching of star formation and thus in quantifying the active and passive galaxies.

A rigorous understanding of the formation of first stars and galaxies from the primordial metal poor gas at the end of cosmic dawn has been a challenge (e.g. Greif et al. 2010). The behaviour of star formation at high redshift is markedly different from that at low redshift. The high redshift galaxies are compact and the SFR for a particular mass, or equivalently the specific SFR increases with redshift (e.g. Shibuya et al. 2015; Sharma et al. 2016). Furthermore, the simulations often find that the star formation at the beginning is abrupt and features episodes of high activity followed by periods of quiescence (e.g. Sharma et al. 2016; Ceverino et al. 2017).

In this work, we investigate the star formation in galaxies in the EAGLE simulation (Schaye et al. 2015; McAlpine et al. 2016). In particular, we draw a comparison between the behaviour of star formation in high redshift haloes and in low redshift haloes. We also discuss the implications of the nature of star formation in high-redshift galaxies for the epoch of reionization and for the population of metal poor stars in the Milky Way.

2. The evolution of the star formation in galaxies

The models of galaxy formation aim to derive the star formation and its evolution over the cosmic ages. Most of these models rely on an interplay of gas accretion, formation of stars and mass ejection by outflow i.e. feedback (e.g. Bouché et al. 2010; Davé et al. 2012; Lilly et al. 2013; Neistein & Dekel 2008; Dekel et al. 2013; Dekel & Mandelker 2014). In these models, coupled equations for the rate of change of stellar mass due to star-formation and rate of change of gas mass due to accretion, star-formation and outflows are solved to model the evolution of galaxies with redshift.

Recently we proposed the $I\kappa\epsilon\alpha$ model that introduces a new method of deriving the salient features of galaxy evolution such as the evolution of the SFR, existence of the main sequence of star formation and the stellar mass function of galaxies, purely from the energy arguments (Sharma & Theuns 2020). The galaxies are virialized systems, therefore the addition of matter through cosmological accretion makes them even more bound as their total energy decreases. However, they compensate for it by forming stars that raise the internal energy. This mechanism is analogous to the behaviour of main sequence stars which also are in virial equilibrium and any decrease in total energy via cooling is compensated by the nuclear energy generation. In galaxies the accretion plays a similar role as the cooling plays in stars so as to make the system even more bound, and the star formation plays the role of nuclear fusion.

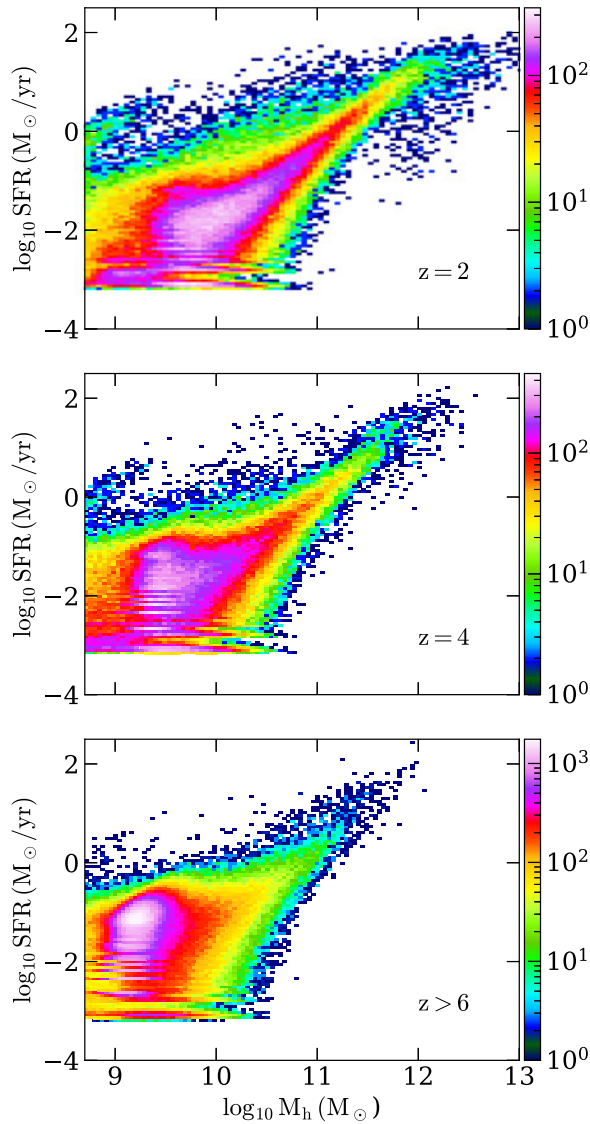


Figure 1. The distribution of star formation rates (SFR) and halo masses (M_h) of galaxies in the EAGLE simulation (Schaye et al. 2015; McAlpine et al. 2016) at redshift $z > 6$ (bottom panel), $z = 4$ (middle panel) and at $z = 2$ (top panel). In the top panel corresponding to $z = 2$, most of the galaxies are distributed along a diagonal ridge indicating the main sequence of galaxies. However at high redshift (bottom panel), most of the galaxies are concentrated in a narrow range of M_h and SFR due to the bursty nature of star formation.

In the $I\kappa\epsilon\alpha$ model the $\text{SFR} \propto M_h^{5/3}$ and the proportionality constant and M_h are redshift dependent (Sharma & Theuns 2020). The redshift dependence is almost the same for different halo masses (e.g. Correa et al. 2015). Given the relation between the SFR and halo mass, and further considering the existence of a relation between halo mass and stellar mass (e.g. Behroozi et al. 2013), it is easy to explain the existence of the main sequence of galaxies at low redshifts (see the top and the middle panel in Fig. 1).

At what redshift the main sequence emerges? The same question can also be stated as whether the evolution and behaviour of star formation at high redshift is the same as at

low redshift. When looking at the bottom panel in Fig. 1 for redshift $z > 6$, we notice that there is a minor hint of the main sequence trend, but it is eclipsed by an exceptionally high SFR in galaxies of a specific halo mass. This indicates that the infant galaxies at high redshift have an abrupt behaviour of star formation.

3. The bursty star formation in first galaxies

The nature of star formation is strikingly different at high redshift, that cannot and should not be described by the smooth evolutionary models, which are more suited at low redshifts to explain the trends such as the main sequence. The high redshift galaxies have higher SFRs (Shibuya et al. 2015; Sharma et al. 2016), and more importantly the star formation is very bursty. This is also apparent in Fig. 1. At low redshifts (top and middle panel) the galaxies occupy a ridge in the SFR – M_h plane that can be identified as the main sequence. Clearly the main sequence is quite well established at redshift 2 (top panel) while it is still developing when looking at redshift 4 (middle panel). At redshift > 6 (bottom panel) there is only a hint of the main sequence at best. Instead a high concentration of galaxies around a halo mass of $\approx 10^9 M_\odot$ and SFR $\approx 0.1 M_\odot \text{ yr}^{-1}$ is clearly evident. This is an indication of a characteristic halo mass in which the star formation history begins with a (most-probable) SFR of roughly $0.1 M_\odot \text{ yr}^{-1}$ that can be understood as the characteristic SFR of the initial burst.

A newly formed galaxy acquires primordial gas, and it begins its journey at the onset of the first burst of stars. The first burst has a huge effect on a tiny infant galaxy as it clears almost all of its gas (see Fig. 2 in Sharma et al. 2018 and Fig. 4 in Sharma et al. 2019). As a result, the SFR is drastically reduced to almost zero. Then after a period of no activity the gas builds up again and the next burst begins, however it is likely that the second burst is not as powerful and damaging as the first one, because the dark matter halo mass and the stellar mass of the galaxy and hence the specific SFR would be lower during the second and subsequent bursts. The cycle is repeated, and with each subsequent burst the galaxy keeps on growing. Slowly and steadily its SFR transforms from being dominated by bursts to a smooth evolution.

4. Implications of bursty star formation

The smooth evolution of star formation driven by cosmological accretion leads to the emergence of main sequence of star forming galaxies in the present day Universe. Then what could be the consequences of the bursty nature of star formation? In the following, we discuss two of the major consequences.

Most of the stars that we see in the present day galaxies (e.g. the Sun), exhibit signatures of all the elements from helium to iron in their spectra. However, finding stars that lack these elements has been a challenge (e.g. Beers & Christlieb 2005). The old stars which lack heavy elements supposedly formed in first galaxies when the Universe was metal (heavy elements) free. The metals are produced in subsequent cycles of star formation.

A subset of metal poor stars detected in our Galaxy shows unusual enhancement of carbon, characterised by carbon enhanced metal poor (CEMP) stars can be further classified into CEMP-no (that lack slow or rapid neutron capture process elements) and CEMP-s (those with abundance of slow neutron capture process elements such as Ba) (Aoki et al. 2007; Frebel et al. 2006; Frebel & Norris 2015).

Most of the normal stars acquire their metals through either the SNe or through the AGB nucleosynthesis channel, and presumably in a well mixed interstellar medium that was replenished from multiple cycles of star formation. However, the CEMP stars likely formed in interstellar medium of first galaxies, because those galaxies had a poorly

mixed interstellar medium due to bursts. Therefore stars could form from gas enriched predominantly by a single enrichment channel, either via the metal-poor SNe-type-II channel or via the AGB channel, the former can produce the CEMP-no stars and the latter can result into the formation of the CEMP-s stars (Sharma et al. 2018).

In a burst, stars are formed with a range of masses and lifetimes. The low-mass ones have long lifetimes while the high-mass ones are short-lived. Therefore the CEMP stars we see today are the low mass stars formed during the initial bursts.

Their high-mass counterparts had short lifetimes. They provided most of the ionizing photons that reionized the Universe. As we see in the bottom panel of Fig. 1, bursts were more likely to occur in the low-mass haloes ($\approx 10^9 M_{\odot}$), but the corresponding galaxies were not the faintest. Hence at high redshift, the bursty brighter galaxies that were hosted by low-mass haloes were the major contributors of the ionizing photons (Sharma et al. 2016, 2017). These bursty galaxies can be investigated in detail by the JWST (Gardner et al. 2006).

5. Acknowledgments

We acknowledge the Virgo Consortium for making their simulation data available. The EAGLE simulations were performed using the DiRAC-2 facility at Durham, managed by the ICC, and the PRACE facility Curie based in France at TGCC, CEA, Bruyères-le-Châtel. We thank IIT Bhilai and the department of science and technology (DST), India, for providing the support to carry out this research. We also thank the IAU for supporting the presentation of this work. We thank an anonymous referee for constructive comments.

References

- Aoki W., Beers T. C., Christlieb N., Norris J. E., Ryan S. G., Tsangarides S., 2007, *The Astrophysical Journal*, 655, 492
- Beardsley A. P., et al., 2019, *PASA*, 36, e050
- Beckwith S. V. W., et al., 2006, *AJ*, 132, 1729
- Beers T. C., Christlieb N., 2005, *ARA&A* , 43, 531
- Behroozi P. S., Wechsler R. H., Conroy C., 2013, *ApJ*, 770, 57
- Bouché N., et al., 2010, *ApJ*, 718, 1001
- Bromm V., 2013, *Reports on Progress in Physics*, 76, 112901
- Ceverino D., Glover S. C. O., Klessen R. S., 2017, *MNRAS*, 470, 2791
- Correa C. A., Wyithe J. S. B., Schaye J., Duffy A. R., 2015, *MNRAS*, 450, 1514
- Crain R. A., et al., 2015, *MNRAS*, 450, 1937
- Davé R., Finlator K., Oppenheimer B. D., 2012, *MNRAS*, 421, 98
- Dekel A., Mandelker N., 2014, *MNRAS*, 444, 2071
- Dekel A., Zolotov A., Tweed D., Cacciato M., Ceverino D., Primack J. R., 2013, *MNRAS*, 435, 999
- Dodelson S., 2003, *Modern cosmology*
- Frebel A., Norris J. E., 2015, *ARA&A* , 53, 631
- Frebel A., et al., 2006, *The Astrophysical Journal*, 652, 1585
- Gardner J. P., et al., 2006, *Space Sci. Rev.*, 123, 485
- Greif T. H., Glover S. C., Bromm V., Klessen R. S., 2010, *The Astrophysical Journal*, 716, 510
- Lilly S. J., Carollo C. M., Pipino A., Renzini A., Peng Y., 2013, *ApJ*, 772, 119
- McAlpine S., et al., 2016, *Astronomy and Computing*, 15, 72
- Mesinger A., Furlanetto S., Cen R., 2011, *MNRAS*, 411, 955
- Naab T., Ostriker J. P., 2017, *ARA&A* , 55, 59
- Neistein E., Dekel A., 2008, *MNRAS*, 383, 615
- Pritchard J. R., Loeb A., 2012, *Reports on Progress in Physics*, 75, 086901
- Santos M. G., Ferramacho L., Silva M. B., Amblard A., Cooray A., 2010, *MNRAS*, 406, 2421

- Schaye J., et al., 2015, *MNRAS*, **446**, 521
- Sharma M., Theuns T., 2020, *MNRAS*, **492**, 2418
- Sharma M., Theuns T., Frenk C., Bower R., Crain R., Schaller M., Schaye J., 2016, *MNRAS*, **458**, L94
- Sharma M., Theuns T., Frenk C., Bower R. G., Crain R. A., Schaller M., Schaye J., 2017, *MNRAS*, **468**, 2176
- Sharma M., Theuns T., Frenk C. S., Cooke R. J., 2018, *MNRAS*, **473**, 984
- Sharma M., Theuns T., Frenk C., 2019, *MNRAS*, **482**, L145
- Shibuya T., Ouchi M., Harikane Y., 2015, *ApJS*, **219**, 15
- Sokasian A., Abel T., Hernquist L. E., 2001, *New A*, **6**, 359
- Springel V., et al., 2005, *Nature*, **435**, 629
- Vogelsberger M., et al., 2014, *Nature*, **509**, 177
- Weltman A., et al., 2020, *PASA*, **37**, e002
- Wise J. H., Demchenko V. G., Halicek M. T., Norman M. L., Turk M. J., Abel T., Smith B. D., 2014, *Monthly Notices of the Royal Astronomical Society*, **442**, 2560
- Yoon J., et al., 2018, *ApJ*, **861**, 146
- van Haarlem M. P., et al., 2013, *A&A*, **556**, A2

Discussion

KATSIANIS: Hello, I enjoyed your talk. Very nice. It has been found that cosmological simulations like EAGLE and IllustrisTNG suffer from resolution limitations (one may run the model at another resolution and get different results if feedback prescriptions are not changed). This raises the question if the models are physical or they are just very well tuned. For example the gas phase metallicity relation even at $z \approx 0$ from EAGLE is different between the high resolution and average (reference) resolution runs. The SFRs of TNG are different between the TNG300 and TNG100 runs besides that the model was tuned to reproduce the CSFRD at the reference resolution. How can we trust that $I\kappa\epsilon\alpha$ is reproducing realistic results since it was tuned to reproduce properties from a simulation that has these limitations. Are there any other observables that the model can reproduce and do you have in mind to check against something specific?

SHARMA: Hi, yes the model does reproduce the SFRs in haloes e.g. the Milky Way that we compared in [Sharma & Theuns \(2020\)](#). We compared the mass-metallicity relations as well with observations. Further, we also predicted the low mass end of the SHMF. Because the model is based entirely on an energy/virial argument, the parameters in the model are not the same as that in the simulation. In fact, one would notice that the outflow feedback is an output of our model, not an input. As for the main sequence, we compared with the main sequence in reference simulation (or automatically with observations as both agree).

The parameters of the model are purely motivated by virial equilibrium argument. Those parameters wouldn't have a unique relation with the implementation of feedback in simulations. So, even if the feedback in the simulation has to be changed with resolution, that would mean that the interpreted relations of that feedback to our $I\kappa\epsilon\alpha$ parameters would be different, but our $I\kappa\epsilon\alpha$ parameters would still be the same.